African Journal of Engineering Research
Vol. 4(3), pp. 43-53, July 2016
ISSN: 2354-2144
Full Length Research Paper

Absorbed power by human body inside high voltage substations under live working conditions

Samy M. Ghania

University of Jeddah, KSA.

Accepted 15 June, 2016

ABSTRACT

The probable risk of electromagnetic fields produced inside high voltage substation is still considered as a competitive topic for utility designers and biomedical field researchers. Hence, the electromagnetic field levels and their induction inside human body should be pre-evaluated as early as the design stage of the substation. This paper deals with the computation of the electromagnetic fields inside a typical high voltage 500/220 kV air-insulated substation (AIS). The typical high voltage substation is simulated by developing multi-scripts of m-file Matlab software package to calculate both of electric and magnetic field individually. Moreover, analytical human body is simulated and allocated within the highly exposure zones of electromagnetic fields. The electromagnetic field induction inside the human body during live working conditions at different accessible positions is evaluated based on the power density vector (poynting vector) using the finite-difference time-domain (FDTD) method for solving Maxwell's equations.

Keywords: High voltage substations, electromagnetic fields inductions, power density vector (poynting vector), FDTD method.

E-mail: Samy_ghania@yahoo.com, sghania@uj.edu.sa.

INTRODUCTION

Power frequency electromagnetic fields produced underneath power lines and inside different electrical installations are still expectedly having much weight of contributions for the exposure risk to living organisms.

This concern is due to the probable interactions with the living organisms for the public and residential areas which still draw worldwide attention because of the results of a number of laboratory and epidemiological studies which indicated possible harmful effects (Batron et al., 1993; Maruvada, 1993). The magnetic fields are produced in many different environments where carrying-current conductors exist such as in the case of electric power transmission and distribution overhead lines, cables and substations. Many studies were performed to study the magnetic fields produced by the electric power transmission lines and electric power substations (Munteanu et al., 2009a, 2009b, 2009c, 2010; Farag et al., 1995; Safigianni and Tsompanidou, 2003; Baraton et al., 1993; Farag et al., 1998). The potential hazards and biological effects of the magnetic fields on the human health were addressed in many studies (Maruvada and Goulet, 1995; Mahmoud et al., 2003). Several countries are following the guidelines given by the International Commission on Non-Ionizing Radiation Protection which sets a value of 100 µT (1000 mG) for 50 Hz magnetic field exposure for the general public and 500 µT (5000 mG) for occupational exposure; therefore, utilities are aware that the public's concerns about this issue are widespread and sincere (Said et al., 2004). The SUBCALC program is commonly used to model the magnetic fields in the 230 kV substation and it shows maximum value of about 30 µT most likely underneath the lower voltage bus bar (Habiballah et al., 2003).

The current paper presents not only the simulation results of two typical 500/220 kV and 220/66 kV to calculate the magnetic field distribution inside each substation but also presents measurement of the magnetic fields inside the same substation existing in Egypt. The measurement of magnetic field is performed using an advanced field meter; HI 3604 ELF survey meter (HI 3604 ELF Survey Meter User's Manual, 2002; HI-4413 Fiber Optic RS-232 Interface With Probe View™

3600 User's Manual).

SYSTEM CONFIGURATIONS

Two typical high voltage substations are simulated using the Matlab – M-Script developer based on Biot-Savart Law in its general form using the (3 D) technique. The actual shape of each section (Ingoing, Higher voltage bus bar, Lower voltage bus bar and Outgoing) of the whole current- carrying conductor system is divided into a number of connected series current segments to closely fit the shape of the section and consequently forms the whole substation conductor system. The start point of calculation (o) is underneath the central phase of higher voltage bus bar. Different configurations of the 500/220 kV and 220/66 kV substation are considered as shown in Figures 1 and 2, respectively. The different configurations are:

i) Single/double bus bar system with horizontal configurations
ii) Double bus bar system with horizontal/vertical configurations

The different scenarios for the bus bar arrangements and their main dimensions and parameters are presented in Figure 3. There are five different scenarios for the bus bar arrangement and these scenarios are:

a) Single bus bar with horizontal arrangements for 500/220 kV
b) Double bus bar with horizontal arrangements for 500/220 kV
c) Double bus bar with horizontal arrangements for 220/66 kV
d) Double bus bar with vertical arrangements for 220/66 kV
e) Double bus bar with all vertical arrangements for 220/66 kV

Figure 2 presents the horizontal and vertical configurations for 220/66 kV substation.

MAGNETIC FIELD CALCULATION

The magnetic field calculation techniques can be classified basically into two types. The first type is a two-dimensional (2 D) technique at which the power conductors are assumed to have infinitely long segments which are parallel to each other's and to a flat ground. The second type is a three - dimensional (3 D) technique at which the power conductors are divided into a finite number of segments which are positioned in space to closely fit the actual shape of the whole conductor system configuration. A three-dimension technique is used as the base of the present magnetic field calculation (Anis et al., 1995). Figure 4 presents an arbitrary current-carrying conductor segment $(\vec{a})$ in free space with respect to reference point (O) and any random observation point (P). For the current segment $(\vec{a})$ current- carrying of current density $(\vec{J})$, the magnetic field intensity is presented in Equation (1) and with integrating over the volume it can be given as in Equation 2.

$$\left\{ \overrightarrow{H} = \left(\frac{1}{4\pi} \int_{v} \frac{\vec{J} \times \vec{Z}_{rr}}{\left| r - \vec{r} \right|^2} dv \right) \right\} \quad (1)$$

$$\overrightarrow{H} = \left(\frac{\vec{I}}{4\pi} \right) \left(\frac{\vec{c} \times \vec{a}}{\left| \vec{c} \times \vec{a} \right|^2} \right) \left| \left(\frac{\vec{a}.\vec{c}}{\left| \vec{c} \right|} - \frac{\vec{a}.\vec{b}}{\left| \vec{b} \right|} \right) \right. \quad (2)$$

Where :
$\vec{J}$: The current density in the current segment. ,
$\vec{Z}_{rr}$: The direction vector between the segment and (p)
I: The current in the segment and a, b and c are vectors shown in

The magnetic flux density due to the n^{th} current segments is:

$$\vec{B}(n) = 0.1\vec{I} \left(\frac{\vec{c} \times \vec{a}}{\left| \vec{c} \times \vec{a} \right|^2} \right) \left(\frac{\vec{a}.\vec{c}}{\left| \vec{c} \right|} - \frac{\vec{a}.\vec{b}}{\left| \vec{b} \right|} \right) \ \mu \text{ Tesla} \quad (3)$$

Then for power line of (M) conductors, the components of magnetic flux densities and its total magnitude value can be given:

$$\begin{aligned} \vec{B}_x &= \sum_{m=1}^{M} \vec{B}_x(m) \\ \vec{B}_y &= \sum_{m=1}^{M} \vec{B}_y(m) \quad \mu \text{ Tesla} \\ \vec{B}_z &= \sum_{m=1}^{M} \vec{B}_z(m) \end{aligned} \quad (4)$$

$$B_{rms} = \sqrt{B_x^2 + B_y^2 + B_z^2} \quad \mu \text{ Tesla} \quad (5)$$

SIMULATION RESULTS

500/220 kV substation

Figure 5 presents the magnetic field distribution over the entire area of the 500/220 kV substation with single bus bar configuration (Scenario A) while all outgoing 220 kV

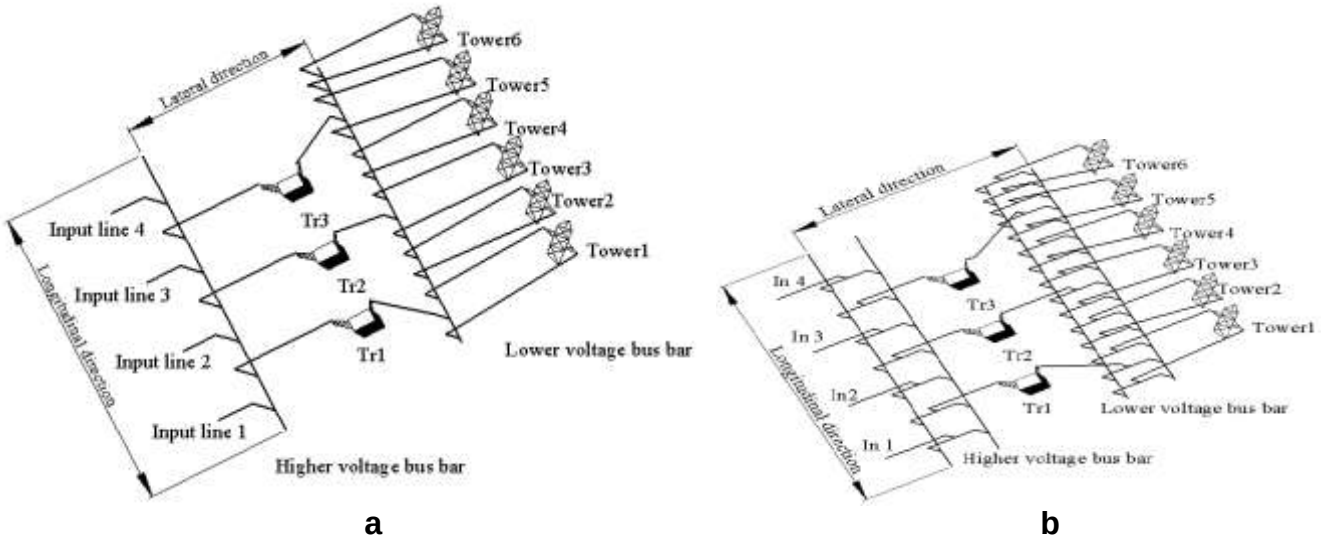

Figure 1. Single line diagram for 500/220 kV substation with single/ double bus bar configuration - Phase A (not to scale). (a) Single horizontal. (b) Double horizontal.

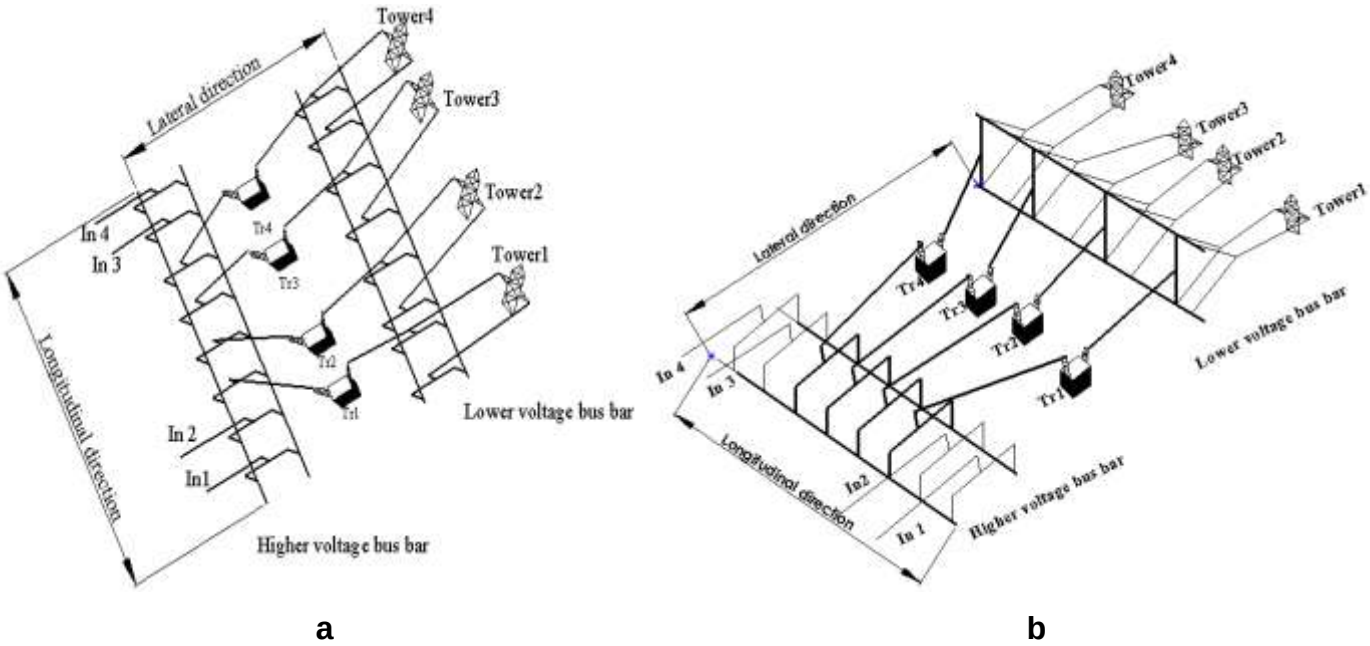

Figure 2. Single line diagram for 220/66 kV substation with double bus bar configuration - Phase A (Not to scale). (a) Horizontal. (b) Vertical.

power lines are loaded with 50 MW. The maximum magnetic field value is about 8.3 µT and it is obtained within the area of lower voltage bus bar. Figure 6 presents the magnetic field distribution over the entire area of 500/220 kV substation while the second ingoing power line is switched off. The maximum magnetic field value is still the same while the magnetic field distribution under the area of higher voltage bus bar is affected and its value increased by about 5%.

Figure 7 presents the magnetic field distribution over the entire area of the 500/220 kV substation with double bus bar configuration (scenario B) while all outgoing 220 kV power lines are loaded with 50 MW. The maximum magnetic field value is about 13.2 µT and it is obtained within the area of lower voltage bus bar.

Figure 8 presents the magnetic field distribution inside the entire area of 500/220 kV substation with double bus bar configuration while the second ingoing power line is

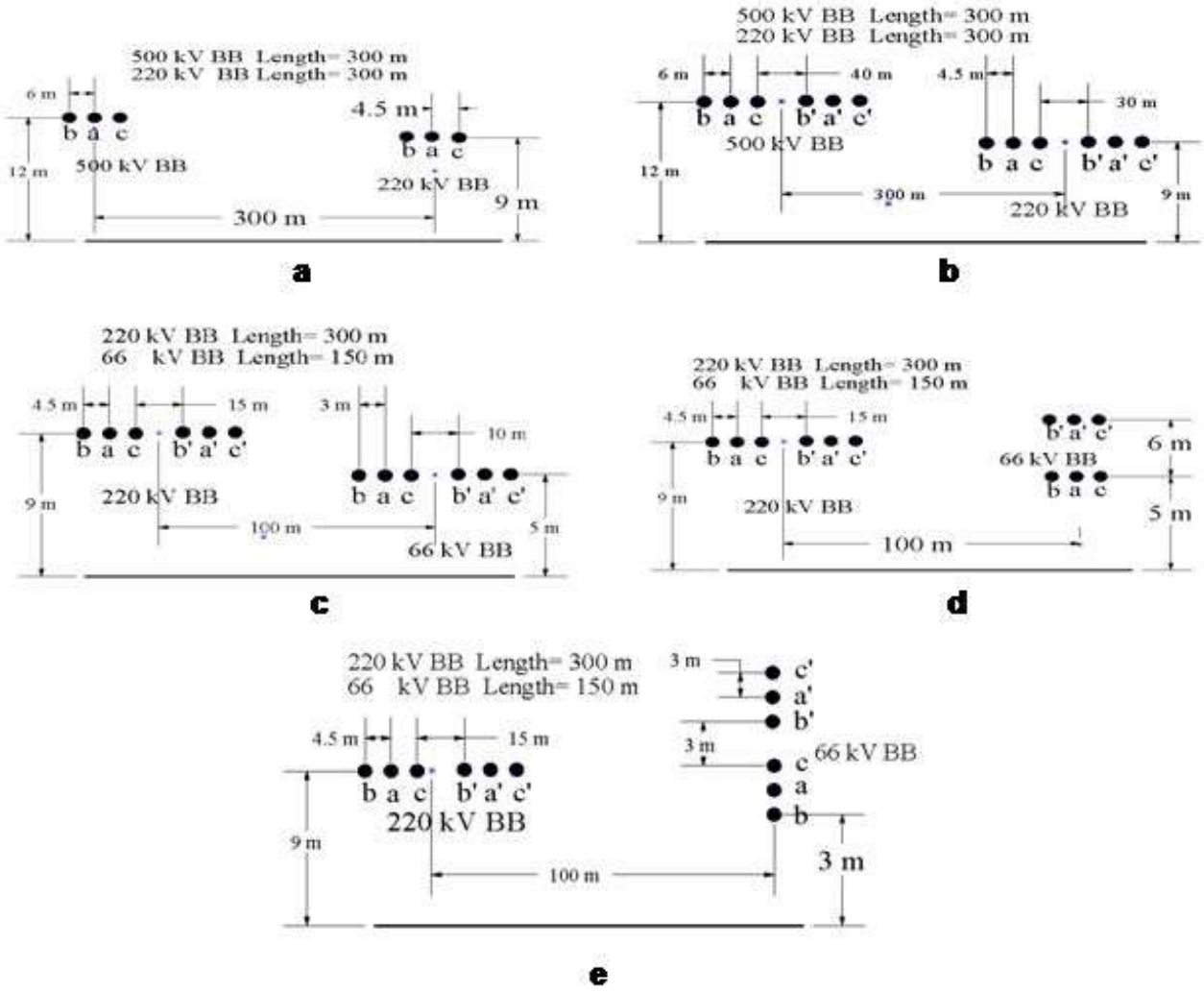

Figure 3. Different scenarios for bus bar arrangements for the simulated substations 500/220 kV and 220/66 kV (Not to scale). (a) Single bus bars for horizontal arrangement 500/220 kV. (b) Double bus bars with horizontal arrangements 500/220 kV. (c) Double bus bars with horizontal arrangements 220/66 kV. (d) Double bus bars with vertical arrangements 220/66 kV. (e) Double bus bars with all vertical arrangements 220/66 kV.

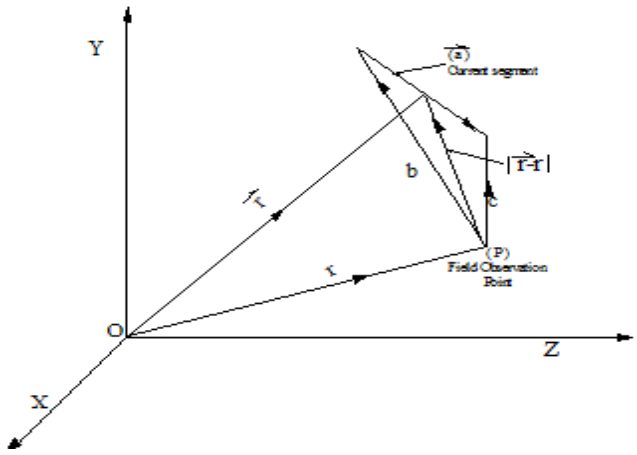

Figure 4. Presentation of current segment in free space.

switched off. The maximum magnetic field value is almost the same while the magnetic field distribution under the area of higher voltage bus bar is affected and its value increased by about 7%.

220/66 kV substation

Figure 9 presents the magnetic field distribution over the entire area of the 220/66 kV substation with double bus bar horizontal configuration (Scenario C) while all outgoing 66 kV power lines are loaded with 25 MW. The maximum magnetic field value is about 31.5 μT and it is obtained within the area of lower voltage bus bar. Figure 10 presents the magnetic field distribution inside the entire area of 220/66 kV substation for the vertical configuration (Scenario D) while all outgoing 66 kV power

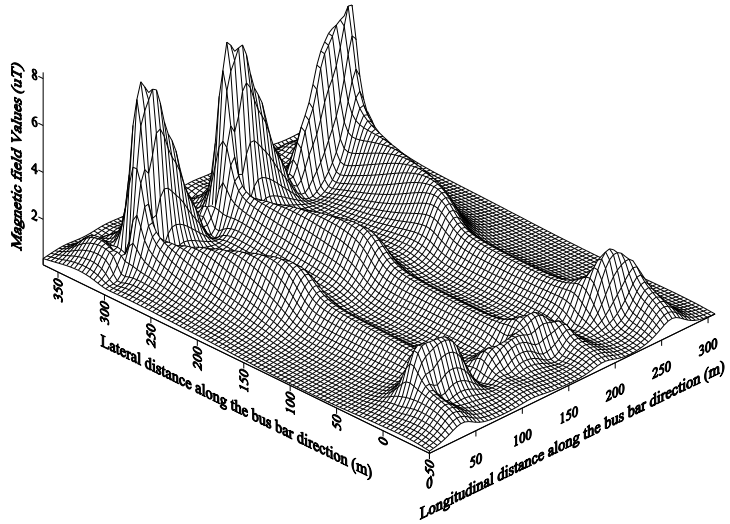

Figure 5. Magnetic field distribution over the entire area of the simulated 500/220 kV substations with single bus bar (Scenario A) configuration and all outgoing lines loaded with 50 MW.

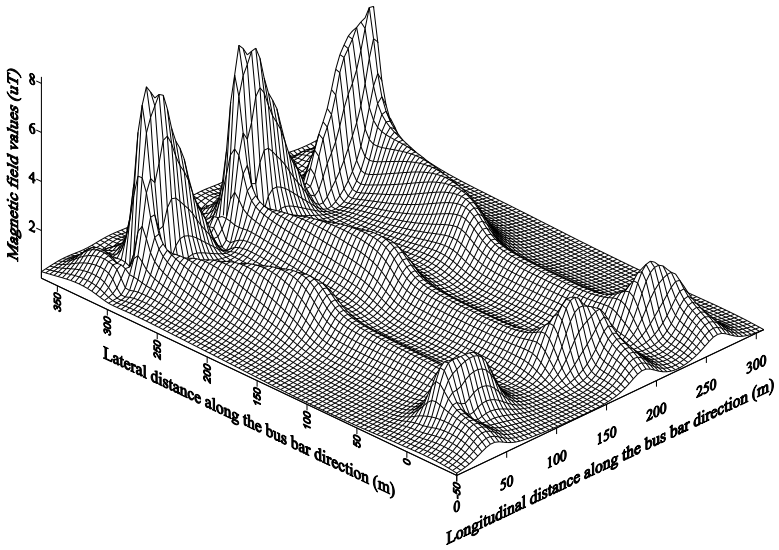

Figure 6. Magnetic field distribution over the entire area of the simulated 500/220kV substations with single bus bar configuration and with one ingoing line off while all outgoing lines loaded with 50 MW.

lines are loaded with 25 MW. The maximum magnetic field value is about 28.4 µT and it is reduced by about 9.8 % from the corresponding horizontal bus bar configuration.

Figure 11 presents the magnetic field distribution over the entire area of the 220/66 kV substation with double bus bar all vertical configuration (Scenario E) while all outgoing 66 kV power lines are loaded with 25 MW.

The maximum magnetic field value is about 7.7 µT and it is obtained within the area of lower voltage bus bar. The maximum magnetic field value is reduced by about 75.5 % from the corresponding horizontal bus bar configuration. Table 1 presents the statistical analysis for the different scenarios for considered bus bars arrangements

MAGNETIC FIELD MEASUREMENTS

For the purpose of simulation results validation, the

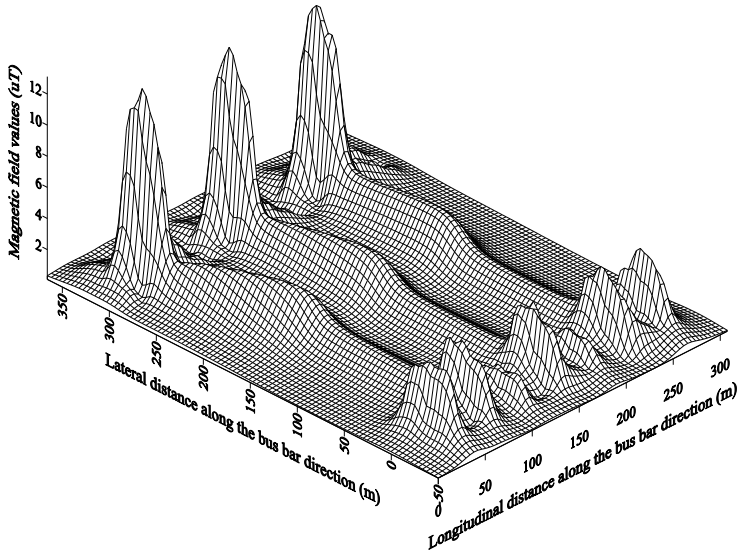

Figure 7. Magnetic field distribution over the entire area of the simulated 500/220 kV substations with double bus bar horizontal configuration (Scenario B) and all outgoing lines loaded with 50 MW.

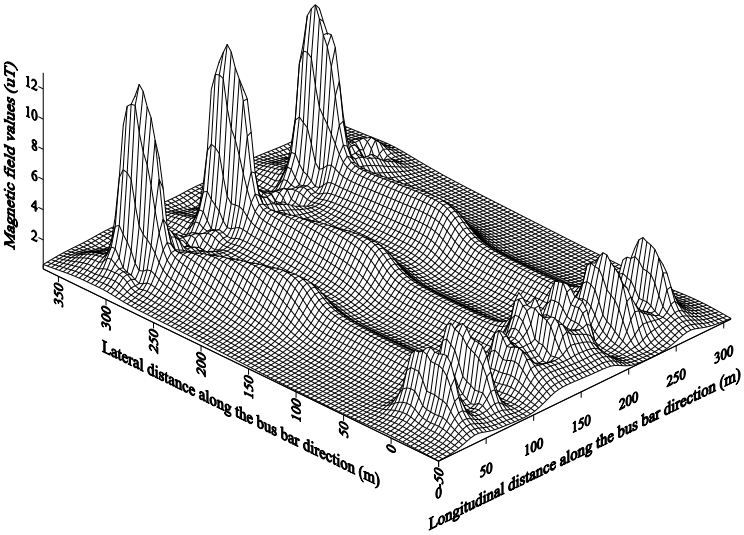

Figure 8. Magnetic field distribution over the entire area of the simulated 500/220 kV substations with double bus bar horizontal configuration and with one ingoing line off while all outgoing lines loaded with 50 MW.

magnetic field measurements are performed at 1 m above the ground surface underneath the lower voltage bus bars inside the two simulated high voltage substation and around the transformers. The measurements are performed with actual loading condition for both 500/220 kV substation allocated in West Cairo while the 220/66 kV substation is allocated in the 10th of Ramadan City in East of Cairo. Both simulated substations are with double bus bar configuration and horizontal bus bar arrangements (Scenarios B and C). The actual loads of the two substations during measurements are presented in Table 2.

Figure 12 presents the calculated and measured magnetic field value longitudinal profiles under the lower voltage bus bar of 500/220 kV substations. The maximum deviation between the calculated and measured values is about 9% which is due to the effects of metallic structure around the bus bars.

Figure 13 presents the calculated and measured longitudinal magnetic field values 1 m away from the

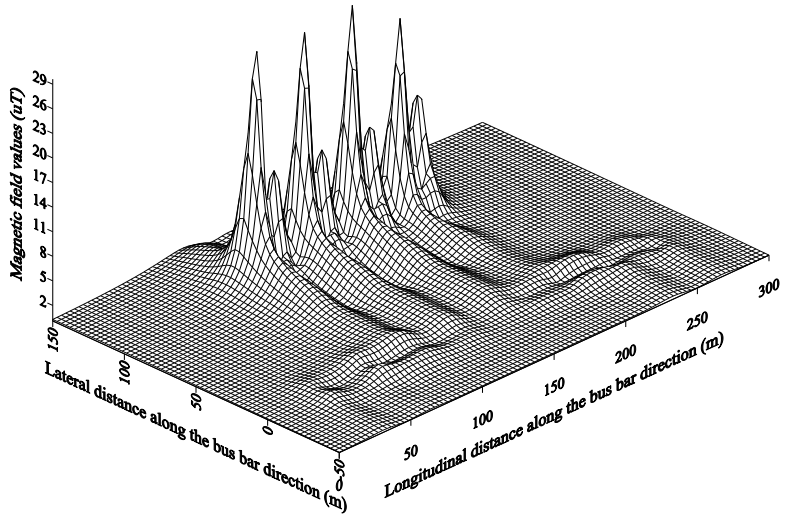

Figure 9. Magnetic field distribution over the entire area of the simulated 220/66 kV substations with double bus bar configuration (scenario C) while all outgoing lines loaded with 25 MW.

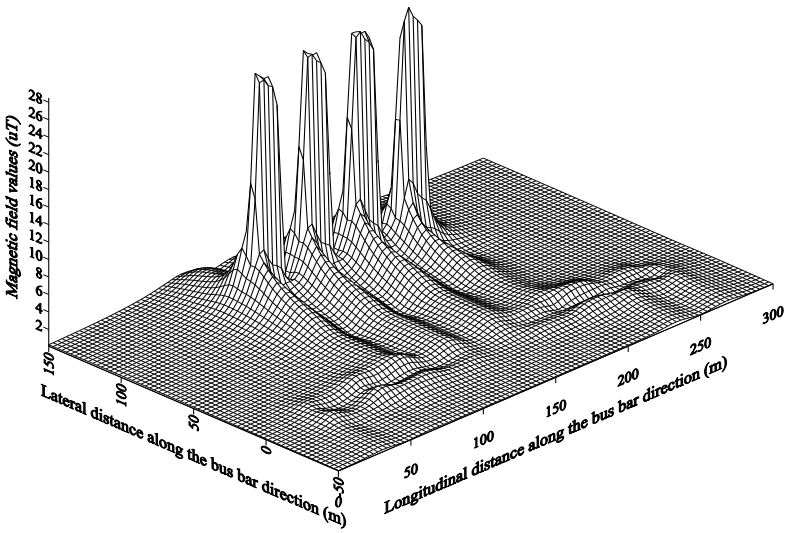

Figure 10. Magnetic field distribution over the entire area of the simulated 220/66 kV substations with double bus bar (scenario D) vertical configuration while all outgoing lines loaded with 25 MW.

transformers under the central phase from the higher voltage bus bar side direction inside 500/220 kV substation with actual loading conditions. It can be noted that the measured magnetic values are higher than the calculated values rather than the scenarios under the bus bars this is because of higher magnetic field values produced by the different transformers windings. The maximum deviation between the maximum measured and calculated magnetic values is about 16% this is because of the high contribution from the transformer windings.

Figure 14 presents the calculated and measured magnetic field value longitudinal profiles under the lower voltage bus bar of 220/66 kV substations. The maximum deviation between the calculated and measured values is about 6% which is due to the effects of metallic structure around the bus bars. Figure 15 presents the calculated and measured longitudinal magnetic field values 1m away from the transformers under the central phase from the lower voltage bus bar side direction inside 220/66 kV substation with actual loading conditions. It can be noted that the measured magnetic values are higher than the

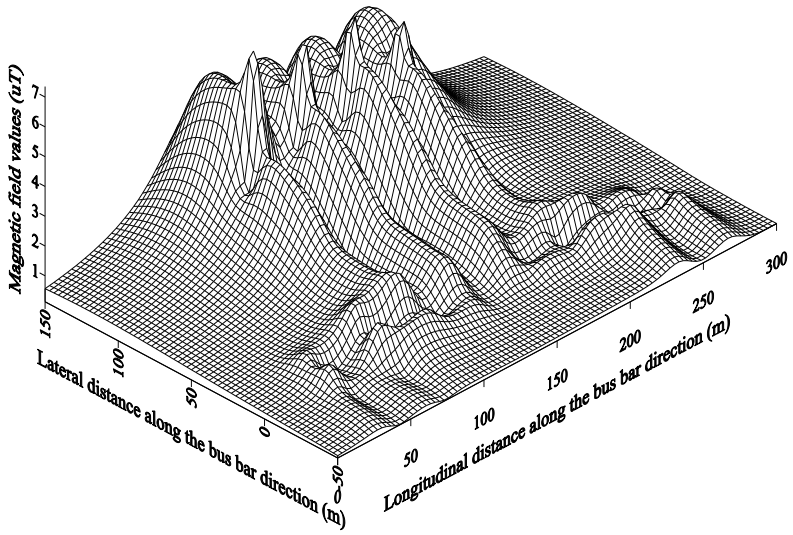

Figure 11. Magnetic field distribution over the entire area of the simulated 220/66 kV substations with double bus bar all vertical configuration (scenario E) while all outgoing lines loaded with 25 MW.

Table 1. Magnetic field statistical values for different bus bar configurations and arrangements.

Bus bar configurations (different Scenarios)	Magnetic field values (uT)			
	Avg	Min	Max	St. dv.
Single bus 500/220 kV bus bar	0.992	0.038	8.2904	0.939
Single bus 500/220 kV bus bar one input off line	1.001	0.038	8.2905	0.949
Double bus 500/220 kV bus bar	1.314	0.069	13.238	1.347
Double bus 500/220 kV bus bar one input off line	1.362	0.074	13.216	1.348
Double bus 220/66 kV bus bar	1.390	0.102	31.578	2.210
Double bus 220kv and 66 kV vertical bus bar	1.350	0.081	28.445	2.947
Double bus 220kv and 66 kV all vertical bus bar	1.585	0.128	7.7115	1.397

Table 2. Actual Loading for the two simulated substations during the measurements.

Actual loads for 500/220 kV substation (MW)											
Tower 1		Tower 2		Tower 3		Tower 4		Tower 5		Tower 6	
C1	C2	C3	C4	C5	C6	C7	C8	C9	C10	C11	C12
47	45	46	48	42	43	47	49	46	47	49	48

Actual loads for 220/66 kV substation (MW)							
Tower 1		Tower 2		Tower 3		Tower 4	
C1	C2	C3	C4	C5	C6	C7	C8
23	24	23	21	24	22	23	21

calculated values rather than the scenarios under the bus bars this is because of higher magnetic field values produced by the different transformers windings. The maximum deviation between the maximum measured and calculated magnetic values is about 25% this is because of the high contribution from the transformer windings.

CONCLUSIONS

Two actual high voltage substations 500/220 kV and 220/66 kV are simulated using the Matlab - M Script developer based on Biot - Savart law in its general form with the three–dimensions technique. The simulated

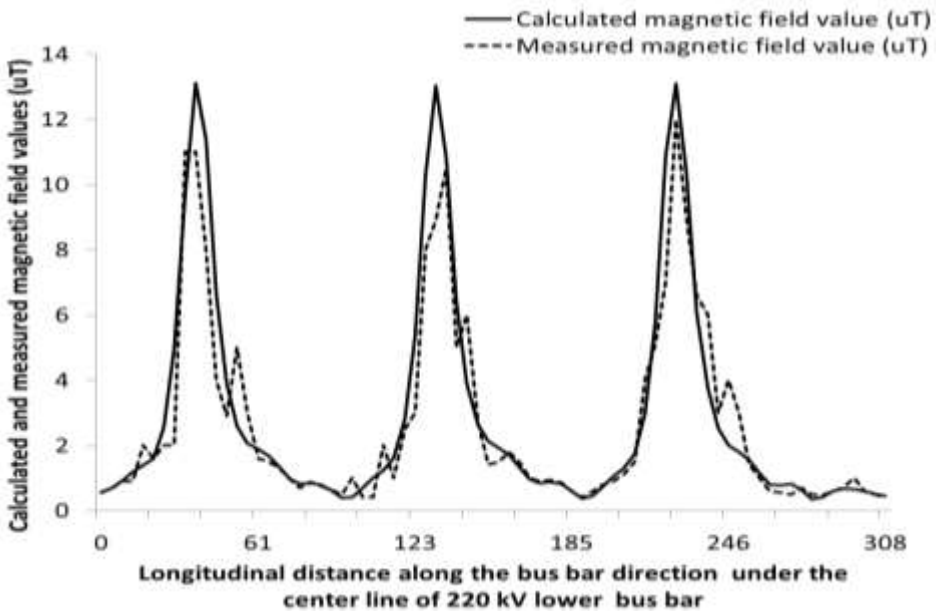

Figure 12. Calculated and measured longitudinal magnetic field profiles under the center line of the lower voltage bus bar inside 500/220 kV substation with actual loading conditions.

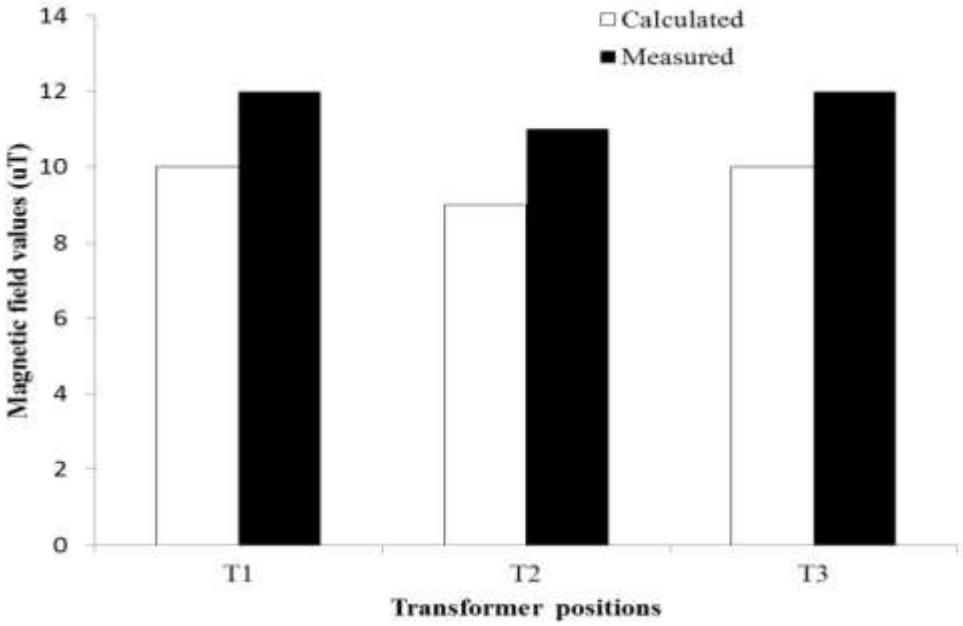

Figure 13. Calculated and measured Longitudinal magnetic field values 1 m away from the transformers under the central phase from the lower voltage bus bar side direction inside 500/220 kV substation with actual loading conditions.

results are compared with actual field measurements at different positions inside the two simulated substations. A good consistence between the measured and calculated magnetic field values under the bus bar area. Meanwhile, the differences between the calculated and measured values show higher deviation around the different transformers because of higher contribution comes up from the higher current inside the transformer windings.

For 500/220 kV substation, the maximum deviation between the measured and calculated magnetic field values is 9% in the area under the bus bars while it reaches 16% around the transformers. For 220/66 kV

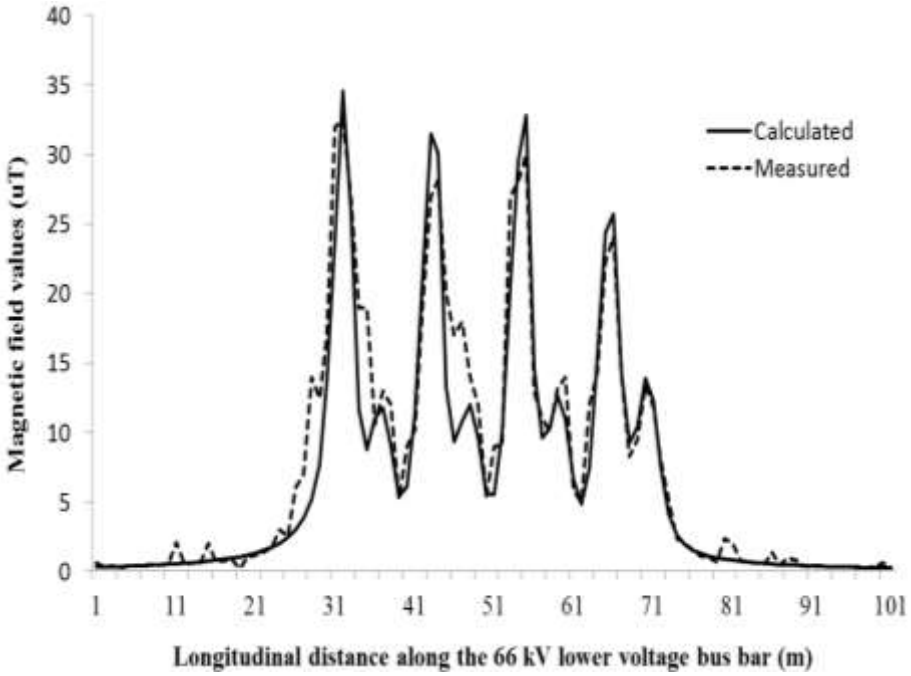

Figure 14. Calculated and measured longitudinal magnetic field profile under the center line of the lower voltage bus bar inside 220/66 kV substation with actual loading conditions.

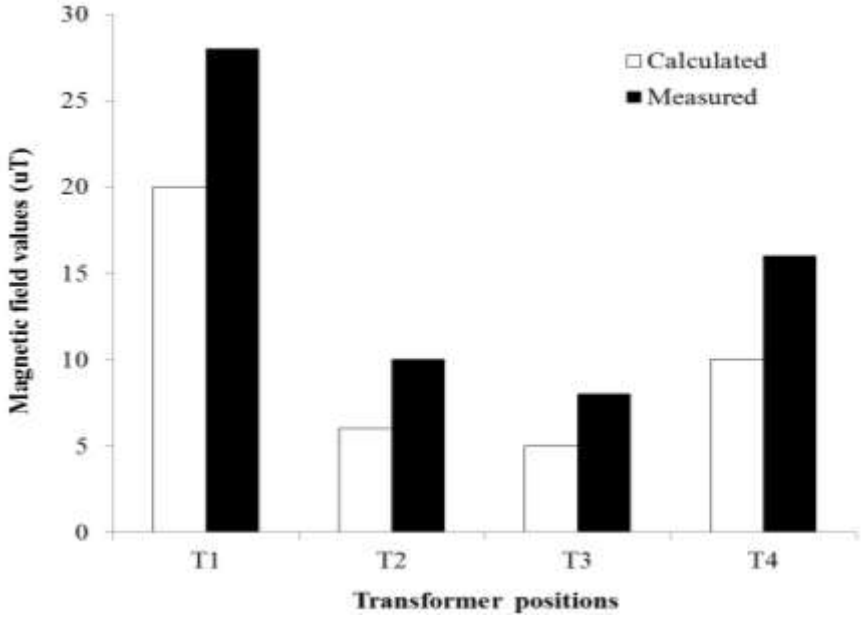

Figure 15. Calculated and measured longitudinal magnetic field values 1m away from the transformers under the central phase from the lower voltage bus bar side direction inside 220/66 kV substation with actual loading conditions.

substation, the maximum deviation between the measured and calculated magnetic field values is 6% in the area under the bus bars while it reaches 25% around the transformers.

REFERENCES

A. S. **Farag**, A. Al-Shehri, J. Bakhashwain, T. C. Cheng (**1995**). Electromagnetic Fields in Substations - Sources Modeling and Measurements. Presented at GCC/CIGRE Sixth Symposium, held in

Bahrain, Oct. 25-26.
A. S. **Farag**, M. M. Dawoud, J. M. Bakhashwain, T. C. Cheng (**1998**). Magnetic Field Measurement and Management in and Around Substations in Saudi Arabia. Cigre, Session 1998, Paris, France.
A. S. **Safigianni**, C. **Tsompanidou**, (**2003**). Measurements of the Electric and Magnetic Fields Due to the Operation of Indoor Power Distribution Substations. 38th International Universities Power Engineering Conference UPEC 2003, Thessaloniki, Greece, September.
C. **Munteanu**, G. Visan, I. T. Pop (**2009c**). Electric and magnetic field distribution inside high voltage power substations. Numerical modeling and experimental measurements. IEEJ Trans Elect Elect Eng, 5(1): 40-45.
C. **Munteanu**, G. Visan, I. T. Pop, V. Topa, E. Merdan, A. Racasan (**2009a**). Electric and Magnetic Field Distribution inside High and Very High Voltage Substations. Proc. 20th International Zurich Symposium on Electromagnetic Compatibility, pp. 277-280, Ian.
C. **Munteanu**, I. T. Pop, G. Visan, V. Topa, A. Racasan, M. Purcar (**2010**). Analysis of the Power Frequency Electric Field Generated by High Voltage Substations. Proc. of the 2010 Asia-Pacific Int. Symposium on Electromagnetic Compatibility, 12-16 April, Beijing, China, pp. 719-722.
C. **Munteanu**, Visan G, Pop IT, Topa V, Merdan E, A. Racasan (**2009b**). Electric and magnetic field distribution inside high and very high voltage substations. Proceedings of the 20th International Zurich Symposium on Electromagnetic Compatibility, pp. 277–280.
H. **Anis**, M. A. Abd-Allah, S. A. Mahmoud (**1995**). Computation of Power Line Magnetic Fields - A Three Dimensional Approach. 9th International Symposium on High Voltage Engineering (ISH1995), paper 8333, Aug/Sept.1995.
Hl 3604 ELF Survey Meter User's Manual, Holladay Ind. 2002.
Hl-4413 Fiber Optic RS-232 Interface With Probe View™ 3600 User's Manual.
I. O. **Habiballah**, M. M. Dawoud, K. Al-Balawi, A. S. Farag (**2003**). Magnetic Field Measurement & Simulation of A 230 kV Substation. Proceedings of the International Conference on Non-Ionizing Radiation at UNITEN (ICNIR 2003) Electromagnetic Fields and Our Health 20th – 22nd October 2003.
I. **Said**, A. S. Farag, H. Hussain, N. A. Rahman (**2004**). Measurement of Magnetic Field from Distribution Substations in Malaysia. Australasian Universities Power Engineering Conference (AUPEC 2004), 26-29 September, Brisbane, Australia.
P. **Baraton**, J. Cahouet, B. Hutzler (**1993**). Three Dimensional Computation of the Electric Fields Induced in a Human Body by Magnetic Fields", 8th The International Symposium on High Voltage Engineering (ISH), Paper 9002, Japan, August 1993.
P. **Batron**, J. Cahouet, B. Hutzler (**1993**). Three Dimensional Computation of the Electric Fields Induced In a Human Body by Magnetic Fields. 8th International Symposium on High Voltage Engineering, (ISH-1993), Paper 9002, Yokohama, Japan, August.
P. **Maruvada**, D. L. **Goulet** (**1995**). Study of population exposure to magnetic fields due to secondary utilization of transmission lines corridors. IEEE Trans Power Delivery, 10(3): 1541-1548.
P. S. **Maruvada** (**1993**). Characterization of power frequency fields in different environments. IEEE Trans. on Power Delivery, 8(2): 598-605.
S. A. **Mahmoud**, A. H. Hamza, S. M. Ghania (**2003**). Residential Exposure to Magnetic fields Produced by High Voltage Transmission Lines. 9th International Middle-East Power Systems Conference, Mepcon, Menoufia, Egypt, December. pp. 745-749.

Citation: S. M. Ghania (2016). Absorbed power by human body inside high voltage substations under live working conditions. Afr J Eng Res, 4(3): 43-53.